

# Effects of Sterilization Methods on the Integrity and Functionality of Covalent Mucin Coatings on Medical Devices

Carolin A. Rickert, Maria G. Bauer, Julia C. Hoffmeister, and Oliver Lieleg\*

Recent advances in the field of biomedical materials have demonstrated that covalent mucin coatings generated on polymeric materials have the potential to greatly improve the surface properties of medical devices such as their wettability, lubricity, and resistance toward biofouling. For such biopolymer-based coatings to be used in a medical application, sterilization of the coated devices is mandatory. However, common sterilization methods such as autoclavation, ethylene oxide fumigation, as well as  $\gamma$  or ultraviolet-irradiation, create harsh conditions during the device treatment, and this might compromise the structural integrity and thus functionality of macromolecular coatings. Here, it is demonstrated that covalent mucin coatings generated on medical devices made from polyvinyl chloride, polyurethane, or polydimethylsiloxane are able to withstand such treatments—albeit to different extents. Among all treatments tested, ethylene oxide fumigation is identified as the most promising method as it maintains the coatings the best. The findings imply that the beneficial properties demonstrated for mucin coatings *in vitro* should indeed be transferable to applications *in vivo*.

neurovascular medicine.<sup>[2,3]</sup> Polydimethylsiloxane (PDMS) is the material of choice for implantable tubes or devices.<sup>[4,5]</sup> However, when those synthetic materials come into direct contact with human tissue or if they remain in the body for a longer time period, complications can arise. The significantly higher stiffness of polymeric materials compared to human epithelia can, for example, entail damage to the tissue during friction processes. The resulting injuries render the tissue more susceptible to infections, which can promote severe inflammations. Moreover, medical devices themselves may constitute a major infection risk, as germs or other contaminants from the environment can attach to the device and are then transported into the human body.<sup>[5,6]</sup>

One strategy to combat these issues is based on the application of coatings to the surfaces of the medical devices.<sup>[7,8]</sup> In


this context, coatings generated from the endogenic macromolecule mucin have been put forward as highly interesting candidates that can provide multiple functionalities at the same time: Covalent mucin coatings were recently shown to efficiently reduce bacterial adhesion to a broad variety of artificial materials,<sup>[9]</sup> to improve the surface wettability,<sup>[10]</sup> to reduce friction,<sup>[11]</sup> and to prevent wear formation on (corneal) tissue under tribological stress.<sup>[12]</sup> Furthermore, by repeatedly reassessing the surface wettability of coated samples, the good stability of such coatings has been proven previously: there, the mucin coatings maintained their functionality very well even when stored for 90 days.<sup>[12]</sup> Mucins are large glycoproteins that constitute an essential part of the inherent immune barrier of mammals.<sup>[13–15]</sup> Here, as the main functional component of mucus, the viscoelastic hydrogel covering all mucosal tissues, mucins not only establish a stable barrier against bacteria and viruses, they also provide excellent lubricity.<sup>[16–18]</sup> From a molecular point of view, the multifaceted properties of mucins are brought about by its complex microarchitecture: the long protein backbone (>5600 amino acids) contains both, a densely glycosylated, hydrophilic core region and two sparsely glycosylated, but partially folded hydrophobic termini.<sup>[19]</sup> A mucin variant commonly used in research is MUC5AC, and decent amounts of this highly functional mucin type can be obtained from porcine stomachs by performing a multi-stage purification process.<sup>[20]</sup> Moreover, these lab-purified mucins have previously been shown to be highly biocompatible<sup>[21]</sup>—both as hydrogels and coatings.<sup>[11,22]</sup> As a purified product of animal

## 1. Introduction

Whether as implants or as tools for invasive procedures or patient care, products made from polymer-based materials are indispensable helpers in many fields of modern medicine. Endotracheal tubes comprising polyvinyl chloride (PVC), for instance, are commonly used in medical emergencies to secure a patient's supply with air.<sup>[1]</sup> Catheters made from polyurethane (PU) have become an integral tool for drainage purposes and to support surgical procedures in cardiovascular, urological, or

C. A. Rickert, M. G. Bauer, J. C. Hoffmeister, O. Lieleg  
TUM School of Engineering & Design  
Department of Materials Engineering  
Technical University of Munich  
Boltzmannstr. 15, 85748 Garching b. München, Germany  
E-mail: oliver.lieleg@tum.de

C. A. Rickert, M. G. Bauer, J. C. Hoffmeister, O. Lieleg  
Center for Functional Protein Assemblies (CPA)  
Technical University of Munich  
Ernst-Otto-Fischer Straße 8, 85748 Garching b. München, Germany

 The ORCID identification number(s) for the author(s) of this article can be found under <https://doi.org/10.1002/admi.202101716>.

© 2021 The Authors. Advanced Materials Interfaces published by Wiley-VCH GmbH. This is an open access article under the terms of the Creative Commons Attribution-NonCommercial License, which permits use, distribution and reproduction in any medium, provided the original work is properly cited and is not used for commercial purposes.

DOI: 10.1002/admi.202101716

origin, however, sterility cannot be guaranteed. Thus, when envisioned to be used as a component of medical devices, mucin-based coatings generated on medical devices need to be sterilized before usage.

Typical examples of standardized procedures suitable for sterilizing medical devices include irradiation with either  $\gamma$  or ultraviolet (UV)-rays, AC, or fumigation with ethylene oxide.<sup>[23,24]</sup> However, all those methods might negatively influence the biochemical integrity of mucin coatings: Thermal stress, for example, often disrupts intramolecular forces that stabilize the conformation of protein domains, and this can entail protein denaturation.<sup>[25]</sup> UV- and  $\gamma$ -irradiation might induce oxidation or cleavage of covalent bonds located in the protein backbone or in aromatic amino acid side chains.<sup>[26,27]</sup> Treatments with ethylene oxide are suspected to modify methionine and cysteine residues in proteins, and this, in turn, can decrease their stability and agglomeration propensity.<sup>[28,29]</sup> To what extent such issues may limit the functionality of covalent mucin coatings is, however, to date unclear.

In this study, we test the integrity and functionality of covalent MUC5AC coatings. Such mucin coatings are generated on medical devices made from PU, PVC, and PDMS and then subjected to different sterilization treatments. By employing two specific detection methods, we show that the glycosylated part of the mucin molecule is more robust toward those physico-chemical challenges than its hydrophobic termini. Contact angle measurements demonstrate that, for nearly all treatments, the hydrophilic character of surfaces coated with

mucins can be maintained to a certain extent. Rotational tribology experiments show that the lubricity provided by mucin coatings is not impaired by any of the sterilization treatments tested here. Lastly, lipid adsorption tests illustrate the superior functionality of coatings subjected to ethylene oxide compared to the other techniques, which underscores the overall finding that this sterilization method has the least impact on the integrity and functionality of the mucin coatings.

## 2. Experimental Section

Unless stated otherwise, all chemicals were purchased from Carl Roth GmbH & Co. KG (Karlsruhe, Germany).

### 2.1. Medical Devices

In this study, mucin coatings were tested on three different medical devices: contact lenses, endotracheal tubes, and urinary catheters (Figure 1a). As described previously,<sup>[12]</sup> the contact lenses studied here (curvature:  $0.07 \text{ mm}^{-1}$ , surface roughness:  $0.66 \pm 0.08 \mu\text{m}$ ) consist of a highly biocompatible, aliphatic Pt-catalyzed liquid silicone based on Si-H and Si-vinyl poly-dimethyl-siloxane (PDMS; Polymer Systems Technology, High Wycombe, UK) without any further additives. They were kindly provided by Woehlk Contactlinsen GmbH (Schönkirchen, Germany). The endotracheal tubes (Super

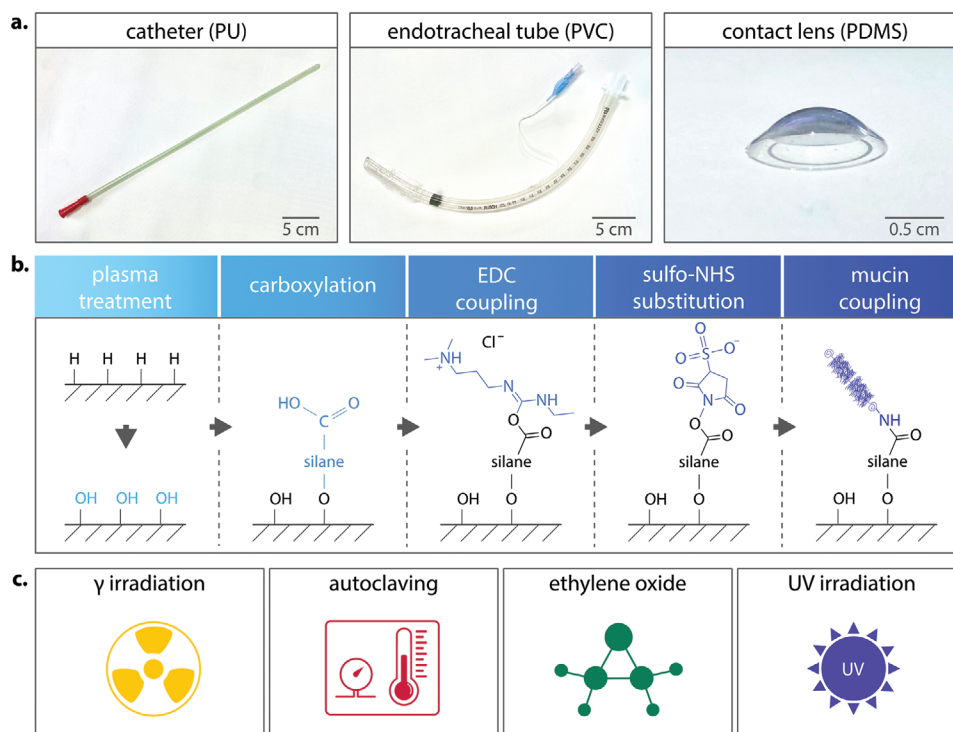


**Figure 1.** Overview of the medical devices, the mucin coating process, and the sterilization techniques used in this study. a) Exemplary images of a urinary catheter (made from PU), an endotracheal tube (made from PVC), and a PDMS-based contact lens as used in this study. b) The coating process employed here starts with plasma activation of the material, followed by carboxylation using a silane precursor, and a final carbodiimide coupling step to covalently attach the mucins onto the surfaces of the medical devices. c) Sterilization of the coated devices was conducted via  $\gamma$ -irradiation, autoclaving, ethylene oxide fumigation, or UV irradiation.

Safetyclear, 10.0 mm, CH40) were purchased from Radecker Notfallmedizin (Ammerbuch/Entringen, Germany) and are made from latex-free polyvinyl chloride (PVC). The urinary catheters (SpeediCath Standard, CH/FR 18/6.0 mm) are fabricated from polyurethane (PU) and were purchased from Coloplast (Hamburg, Germany). To obtain uniform specimens from the latter two medical devices, round samples with a diameter of 7 mm were cut from the endotracheal tubes (curvature of the samples:  $0.1 \text{ mm}^{-1}$ , surface roughness:  $0.4 \pm 0.5 \text{ }\mu\text{m}$ ) and the catheters (curvature of the samples:  $0.17 \text{ mm}^{-1}$ , surface roughness:  $2.3 \pm 0.5 \text{ }\mu\text{m}$ ) using an eyelet press (IstaBreeze Germany GmbH, Bad Rappenburg, Germany). The surface roughness (expressed by the arithmetical mean height  $S_q$  according to ISO 25178-2) of each sample was measured on a laser-scanning microscope (VK-X1000, Keyence, Neu-Isenburg, Germany) equipped with a 20 $\times$  lens (CF Plan, NA = 0.46; Nikon, Chiyoda, Tokyo, Japan). A Gaussian filter with a cut-off wavelength of 0.2 mm was applied before calculating the roughness parameter with the MultiFileAnalyzer software (v2.1.3.89, Keyence). The endotracheal tubes and the urinary catheters are commercial medical products approved for clinical usage in the European market (Conformit  Europ enne, CE) labeled). Before further usage, all samples were first washed in 70% (v/v) ethanol and then in ddH<sub>2</sub>O by incubating them in the respective solution while being placed onto a rolling shaker (RS-TR 05, Phoenix Instrument GmbH; Garbsen, Germany) for 30 min.

## 2.2. Mucin Purification

Porcine gastric mucins (MUC5AC) were manually purified.<sup>[30]</sup> In brief, raw mucus was manually collected from the mucosal tissue of fresh pig stomachs obtained from a local slaughterhouse (Schlacht- und Viehhof, M nchen, Germany). The harvested material was diluted 1:5 in phosphate buffered saline (pH 7.0) containing  $170 \times 10^{-3} \text{ M}$  sodium chloride and 0.04% sodium azide, and then homogenized at 4  C overnight by stirring. To remove mesoscopic impurities and cellular debris, two centrifugation steps ( $17\,590 \times g$  for 30 min and  $158\,306 \times g$  for 1 h) were conducted. Afterward, the mucins were separated from other molecules via size exclusion chromatography using an  KTA purifier system (GE Healthcare, Chicago, IL, USA) equipped with an XK50/100 column packed with Sepharose 6FF (GE Healthcare). The collected mucin-containing fractions were pooled, and 1 M NaCl was added. The mixture was then dialyzed against ultrapure water and concentrated by crossflow filtration using an ultrafiltration hollow fiber cartridge with a molecular weight cut-off of 100 kDa (UFP-100-E-3MA, GE Healthcare). After lyophilization, the mucin was stored at  $-80 \text{ }^\circ\text{C}$ . For further processing, the lyophilized mucin was solubilized in the desired buffer, vortexed for 1 min and kept at 4  C on a shaking incubator (set to 750 rpm) for 2 h to generate a homogeneous solution.

## 2.3. Covalent Mucin Coating Process

The mucin macromolecules were covalently attached to the surfaces of the medical devices by performing a carbodiimide

coupling process (Figure 1b).<sup>[31]</sup> For this purpose, the sample surfaces were first activated by exposing them to plasma generated with ambient air (60 W, 0.4 mbar, 90 s; plasma oven "SmartPlasma 2," plasma technology GmbH, Herrenberg, Germany). Subsequently, surface carboxylation was achieved by incubating the specimens in  $10 \times 10^{-3} \text{ M}$  acetate buffer (pH 4.5) supplemented with 1.0% (v/v) of the coupling agent *N*-[(3-trimethoxysilyl)propyl]ethylenediamine triacetic acid trisodium salt (TMS-EDTA, abcr GmbH, Karlsruhe, Germany) at 60  C for 5 h. To remove loosely bound silanes, the samples were first dipped into iso-propanol (>99.5%) and then washed in 96% (v/v) ethanol on a rolling shaker (70 rpm; RS-TR 05, Phoenix Instrument GmbH, Garbsen, Germany) for 1 h. The generated siloxane bonds were stabilized by baking the samples at 80  C for 2 h (for PDMS samples) or at room temperature for 24 h (for PVC and PU samples). To finally attach the MUC5AC macromolecules via EDC-NHS coupling, the carboxyl groups previously generated on the sample surfaces were activated by incubating the samples in  $100 \times 10^{-3} \text{ M}$  2-(*N*-morpholino)ethanesulfonic acid buffer (MES buffer, pH 5.0) comprising  $5 \times 10^{-3} \text{ M}$  1-ethyl-3-(3-(dimethylamino)propyl)carbodiimide (EDC) and  $5 \times 10^{-3} \text{ M}$  *N*-hydroxysulfosuccinimide (sulfo-NHS, abcr GmbH) for 30 min while moderately shaking (35 rpm). The samples were then immersed into Dulbecco's phosphate buffered saline (DPBS; Lonza, Verviers, Belgium) containing 0.1% (w/v) MUC5AC and kept there at 4  C for 18 h. Last, if not stated otherwise, the coated samples were gently washed in 80% (v/v) ethanol, air-dried, stored in sterilization bags (Medi Pack GmbH, M nchengladbach, Germany), and rehydrated in DPBS for 24 h before each experiment. Importantly, all specimens used in a given set of experiments were coated at the same time and stored for the same duration—independently of whether or not a sterilization process was conducted.

As described earlier, small specimens of the different medical devices were subjected to the covalent coating process—but not whole devices. For other small samples of similar sizes, a uniform density of such mucin coatings was demonstrated in a previous study.<sup>[9]</sup> However, once full-length endotracheal tubes or catheters are supposed to be coated, a suitable technical process needs to be developed and its success (i.e., the uniformity of the coating) needs to be verified.

## 2.4. Sterilization Methods

Four different sterilization methods were conducted (Figure 1c). For autoclaving (AC), sterilization bags (Medi Pack GmbH, M nchengladbach, Germany) containing the dried samples were placed into an autoclave (Systec VX-150, Systec GmbH, Linden, Germany), and a standard sterilizing process (121  C, 20 min) was applied. Treatments with  $\gamma$ -irradiation (dose: 25–50 kGy; system type: JS9000; complied standards: EN ISO 9001, EN ISO 13 485, EN ISO 11137-1) or ethylene oxide (EO; duration: 5 h, temperature: 45  C, pressure 610 mbar, average EO concentration:  $700 \text{ mg L}^{-1}$ ) were conducted by employing commercial standard processes available at the company steripac GmbH (Calw, Germany). Here, the samples were stored in sterilization bags as well. For sterilization via UV irradiation, the samples were directly placed into a petri dish, placed into a sterilization

chamber (BLX-254, Vilber Lourmat GmbH, Eberhardzell, Germany), and exposed to UV irradiation (254 nm, 5 × 8 W) for 30 min. After irradiation, the samples were moved into sterilization bags for further storage.

## 2.5. ELISA

An indirect enzyme-linked immunosorbent assay (ELISA) was conducted that targets the unglycosylated, hydrophobic termini of the surface-bound MUC5AC molecules. Therefore, the PU and PVC samples were used as prepared earlier (round shaped), and the contact lenses were cut into four identical parts to fit into the wells of a 48-well plate. The specimens were incubated in blocking buffer (5% [w/v] milk powder dissolved in DPBS containing 1 mg/mL Tween 20) at 4 °C overnight. Additionally, empty wells of a 48-well plate (one per sample) were blocked using the same blocking buffer. After overnight incubation, all wells were washed with DPBS-Tween, and the samples were transferred into empty, blocked wells. Then, 300 μL of blocking buffer supplemented with a specific antibody for MUC5AC detection (1:400; ABIN966608, antibodies-online GmbH, Aachen, Germany) were added into each well, and the well plate was placed on a shaker (35 rpm) at 4 °C for 1 h. Before adding the secondary antibody, the wells were washed thrice with DPBS-Tween. A horse radish peroxidase (HRP) conjugated goat anti-mouse (murine) IgG antibody (ABIN237501, antibodies-online GmbH) was diluted 1:5000 in blocking buffer, and 200 μL of this solution were added to each sample. Antibody incubation was allowed to take place on a shaker (35 rpm) at 4 °C for 2 h.

After washing the wells with DPBS (without any Tween), 150 μL of QuantaRed Working Solution were added to each well. This solution comprises of 50 parts QuantaRed Enhancer Solution, 50 parts QuantaRed Stable Peroxide, and 1 part QuantaRed ADHP Concentrate (QuantaRed Enhanced Chemifluorescent HRP Substrate Kit 15 159; Thermo Fisher Scientific, Waltham, MA, USA). After 30 min of incubation at RT, 100 μL of the solution were removed from each well and transferred into an empty well plate, and the fluorescence signal created by the converted substrate was quantified using a plate reader (ex.: 540 nm, em.: 590 nm; Fluoroskan Ascent FL, Thermo Labsystems, Waltham, MA, USA). The measured values were normalized to the intensities measured for coated but untreated reference samples (of the respective group).

## 2.6. Lectin Depletion Assay

To complement the ELISA measurements, the presence of surface-bound MUC5AC molecules was probed with a lectin depletion assay that targets the glycosylated, central region of the MUC5AC glycoprotein. For this purpose, coated samples (similar geometries as described for the ELISA assay) were washed thrice with DPBS and placed into wells of a 48-well plate. Then, 300 μL of DPBS containing 12.5 μg mL<sup>-1</sup> fluorescently labeled lectins (FITC conjugated lectin from *triticum vulgare*, wheat, Sigma Aldrich) were added to each well. Those lectins specifically target sialic acids (in detail, *N*-acetylneuraminic acid and *N*-glycolylneuraminic acid) and *N*-acetylglucosamin.<sup>[32]</sup> The

well-plate was placed on a shaker (35 rpm) under light exclusion for 12 h. Afterward, 200 μL of the lectin solution were removed from each well and transferred into an empty well plate. The fluorescence signal obtained from those lectin solutions was then quantified using a plate reader (ex.: 485 nm, em.: 538 nm; Fluoroskan Ascent FL, Thermo Labsystems). The measured values were normalized to the intensities measured for the blank reference samples of each group.

## 2.7. Tribological Measurements

Tribological experiments were conducted on a commercial shear rheometer (MCR 302, Anton Paar, Graz, Austria) equipped with a rotational tribology setup (T-PTD 200, Anton Paar) as described previously.<sup>[33]</sup> In brief, a ball-on-3-pins geometry was established by combining a rotating steel sphere (Ø 12.7 mm, Kugel Pompel, Wien, Austria) with PDMS-pins (Ø 5.5 mm). The cylindrical PDMS-pins were produced by adding one part crosslinker to ten parts of the PDMS prepolymer (PDMS, Sylgard 184, Dow-Corning, Wiesbaden, Germany), placing the mixture into a vacuum chamber for 1 h, pouring the degassed mixture into custom-made molds, and finally curing the pins at 80 °C for 4 h. Before each measurement, the pins were gently washed with 70% (v/v) ethanol and inserted into a pin holder; here, special care was taken to achieve symmetric pin positions (to ensure centric rotation of the ball on the three pins). 600 μL of HEPES buffer (4-[2-hydroxyethyl]-1-piperazineethanesulfonic acid buffer) were then pipetted onto the pin-holder such that the pins were fully covered. The HEPES buffer had a pH of 7.3, which corresponds to the average pH value of the human tear film.<sup>[34]</sup> The temperature control was set to  $T = 20$  °C, which represents the standard storage conditions (room temperature) of such devices. A normal force of  $F_N = 6$  N was applied, which corresponds to a contact pressure of  $\approx 0.35$  MPa (according to Hertzian contact theory).<sup>[35]</sup> Then, friction coefficients were measured for sliding velocities ranging from 10<sup>3</sup> to 10<sup>-2</sup> mm s<sup>-1</sup> (by applying logarithmic speed ramps with ten measuring points per decade; sliding velocities were varied from “fast” to “slow” to minimize stick-slip effects) using an acquisition time of 10 s per data point.

## 2.8. Contact Angle Measurements

To assess the wetting behavior of the different medical devices, contact angle measurements were performed using a drop shape analyzer device (DSA25S, Krüss GmbH, Hamburg, Germany). Therefore, the coated samples were removed from the buffer solution and dried with oil-free pressurized air (Aero Duster 105/2) for  $\approx 3$  s. Uncoated samples were used as described above (see Section 2.1). Afterward, a droplet of 2 μL of ultrapure water was placed onto each sample, and lateral images of the droplets were captured with a high-resolution camera (acA1920, Basler, Ahrensburg, Germany) integrated into the device. These images were processed with the software ADVANCE (AD4021 v1.13, Krüss GmbH) using the integrated ellipse (tangent-1) fit method; static contact angles were defined as the water enclosed angle between the surface and the edge of the droplet.



## 2.9. Assessment of the Break-up Time (BUT)

The BUT quantifies the duration that a liquid film completely covers a surface exposed to air without rupturing. To measure this BUT, contact lenses were hydrated in DPBS overnight. Afterward, the lenses were removed from the liquid, and the excess water was removed by gently blotting the lenses with a low-lint laboratory paper towel, and the lenses were placed onto a dry glass slide. Then, a stopwatch was started immediately, and the time point at which a first rupture of the fluid film appeared was recorded.

## 2.10. Lipid Deposition Tests

To assess lipid deposition on the sample surfaces, a depletion assay was conducted. Therefore, the samples (similar geometries as described for the ELISA assay) were gently washed in 70% (v/v) ethanol and ddH<sub>2</sub>O, and then placed into a 48-well plate. Then, 300  $\mu$ L of DPBS supplemented with  $25 \times 10^{-6}$  M of fluorescently labeled 1,2-dioleoyl-sn-glycero-3-phosphoethanolamine (DOPE-Atto590, ATTO-TEC GmbH, Siegen, Germany) were added to each sample. After an incubation step at 4 °C for 4 h (while gently shaking at 25 rpm), 200  $\mu$ L of the lipid solution were removed from each well and transferred into an empty well plate. The fluorescent signals of those transferred solutions were then quantified using a plate reader (ex.: 584 nm, em.: 620 nm; Fluorskan FL, Thermo Labsystems), and the measured values were normalized to the intensity values measured for an empty well.

## 2.11. Tests for Statistical Significance

To test for normal data distribution, a Lilliefors test was applied; a two-sample F-test was employed to check for equal variances. To test for significant differences between normally distributed samples, a two-sample *t*-test was applied when homogeneity of variances was met, whereas a Welch's *t* test was performed for unequal variances. For samples that were not normally distributed, a Wilcoxon–Mann–Whitney test was performed. All statistical analyses were performed using Matlab (version R2019a, MathWorks, Natick, MA, USA), and differences were considered statistically significant if a *p*-value below 0.05 was obtained.

## 3. Results and Discussion

Covalent coatings with MUC5AC macromolecules were established on samples of three medical devices: urinary catheters (PU), endotracheal tubes (PVC), and contact lenses (PDMS). In a first set of experiments, we aim at assessing the durability of those covalent mucin coatings by probing the structural integrity of mucins after exposing the coated specimens to different sterilization procedures. More precisely, we first employ an antibody-based detection method (ELISA) that specifically targets the non-glycosylated, hydrophobic termini of the MUC5AC glycoproteins (Figure 2a–c).

For all three tested materials, the fluorescence signals obtained after sterilization with either  $\gamma$ -irradiation or autoclavation are significantly lower than those obtained for untreated

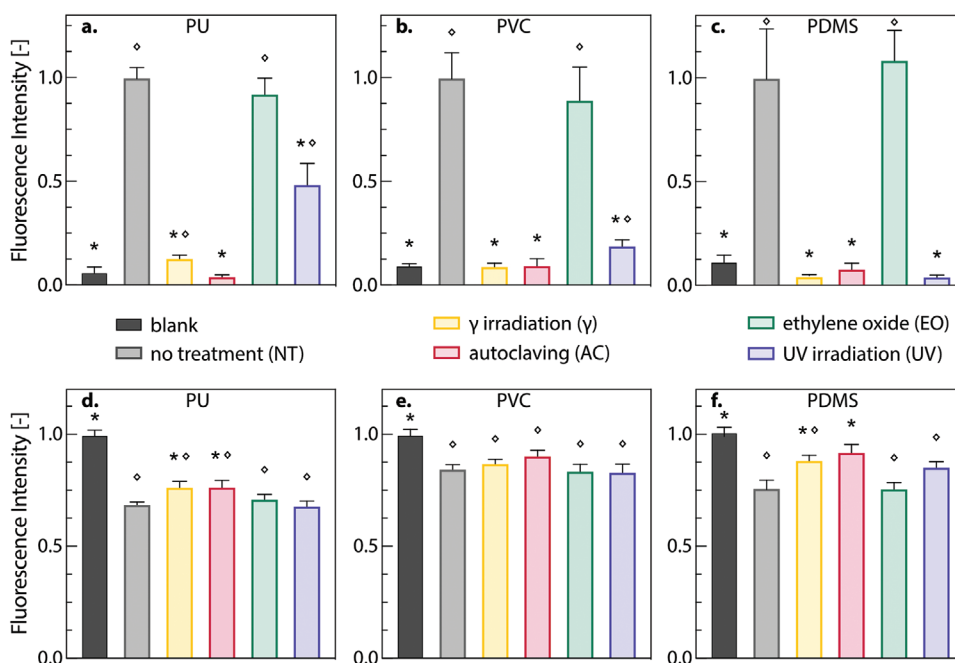


**Figure 2.** Detection of surface-bound mucins MUC5AC via ELISA and lectin-binding. The normalized fluorescence intensities obtained with an ELISA (a–c) and a lectin-based depletion assay (d–f) are shown for different medical devices coated with mucins. The coated samples were either stored without any further treatment, or sterilized via  $\gamma$ -irradiation, autoclavation, ethylene oxide fumigation, or UV irradiation. The error bars denote the standard error of the mean as obtained from  $n \geq 4$  samples. Asterisks and rhombi denote statistically significant differences between a treated sample group and the untreated references or the blank sample, respectively (based on a *p*-value of 0.05).

mucin coatings. In fact, the measured values are comparable to those obtained for a blank sample. This indicates that these two sterilization approaches induce severe damage to or even full cleavage of the hydrophobic MUC5AC termini. The same picture arises for UV irradiated mucin coatings generated on PDMS or PVC. On PU, in contrast, somewhat higher values are obtained for UV irradiated samples; yet, also here, those values are still considerably lower than those obtained for untreated coatings. In marked contrast to those observations, samples that were subjected to ethylene oxide fumigation return fluorescent signals that are similarly high as those determined for untreated coatings—and this assessment applies to coatings generated on any of the three materials. From these tests, we conclude that the integrity of the hydrophobic termini of the mucin molecules is impaired by autoclavation and irradiation with either gamma or UV rays, respectively. In contrast, sterilization with ethylene oxide maintains the integrity of the terminal polypeptide chains.

So far, we focused on the unglycosylated, hydrophobic terminal regions of mucins; however, the glycosylated core region of the MUC5AC constitutes the largest part of the macromolecule and plays a key role for many of the molecule's important properties. Thus, in a next step, the presence and accessibility of this glycosylated part of surface-attached mucins is probed by employing a lectin binding assay that specifically detects a structural motif from the glycosylation pattern of the mucin glycoprotein (Figure 2d–f). Here, the coatings are incubated with a solution of fluorescent lectins, and the lectin solution

is analyzed after this incubation step. Thus, low fluorescence intensity values represent a strong depletion of the lectin molecules and this, in turn, indicates the presence of a high number of glycosylated groups on the mucin coatings. Consistently, for almost all coatings, the obtained values are significantly lower than those obtained for blank, uncoated samples; only for autoclaved mucin coatings generated on PDMS, the measured difference is not significant. Importantly, for all coatings that were sterilized by either ethylene oxide exposure or UV irradiation, the lectin depletion induced by the coatings is equally high as for untreated reference coatings. This is a good indication that, for those particular samples, the density of glycan groups (and thus the glycosylated area in general) in the treated coatings is not affected by the sterilization treatment.

Together, the two assays show that the glycosylated regions of the mucin coatings seem to be more resistant toward the applied sterilization methods than the non-glycosylated terminal regions. This agrees with our expectations since the glycosylation pattern was already observed to protect the protein backbone from proteolytic degradation.<sup>[35]</sup> The terminal, non-glycosylated parts of the polypeptide backbone, in turn, are more vulnerable. Moreover, the results discussed so far suggest that both parts of the MUC5AC glycoprotein seem to survive a treatment with ethylene oxide gas very well. Here, with either assay, no significant differences were observed compared to untreated coatings.

Having probed the structural integrity of the covalent mucin coatings after subjecting them to the different sterilization

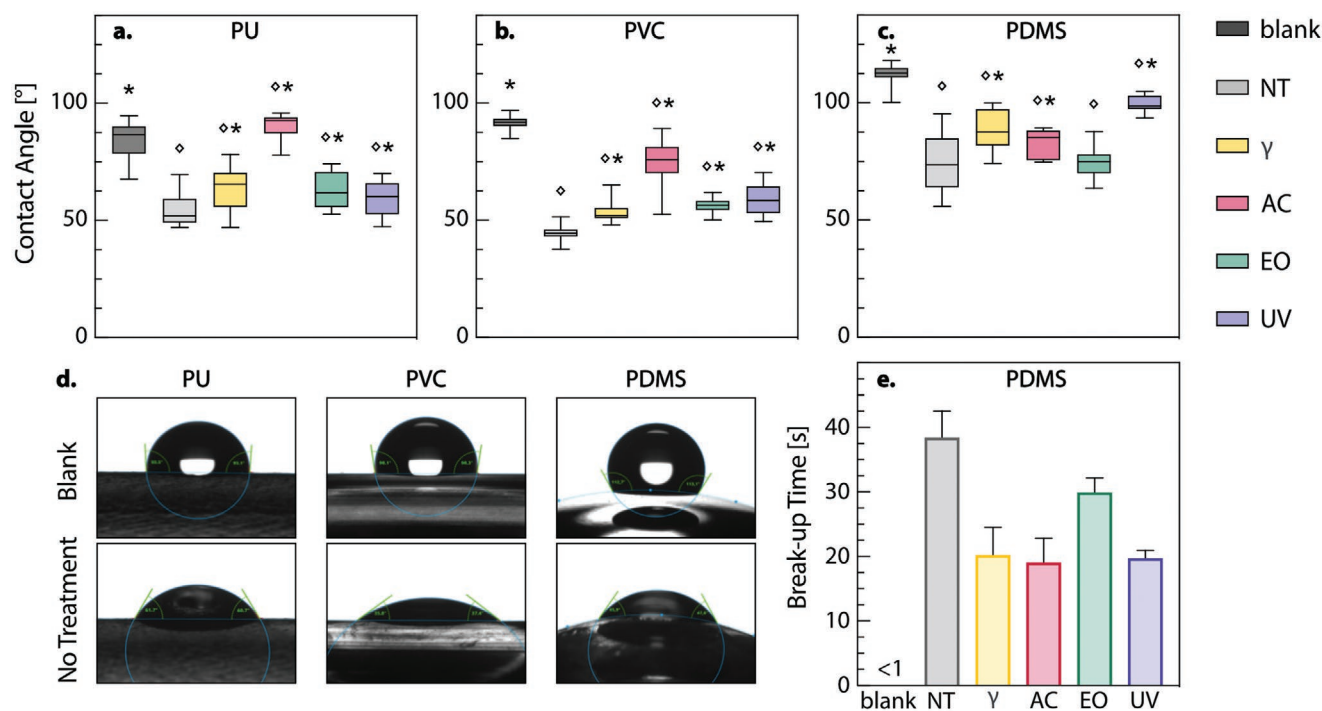


**Figure 3.** Wettability of sterilized mucin coatings generated on different medical devices. Contact angles ( $n \geq 10$ ) quantify the wettability of the surfaces and are displayed for a) PU, b) PVC, and c) PDMS based medical devices. Contact angles larger than  $90^\circ$  denote hydrophobic behavior, whereas values smaller than  $90^\circ$  represent hydrophilic surfaces. Asterisks and rhombi denote statistically significant differences between a treated sample and the untreated reference or the blank sample, respectively (based on a  $p$ -value of 0.05). d) Exemplary images of the three blank device surfaces and the same set of surfaces carrying a mucin coating (that has not been subjected to any sterilization process). e) Break-up times as determined for PDMS-based contact lenses (blank, coated, or coated and sterilized). Error bars indicate the standard error of the mean as obtained from  $n = 3$  samples.

techniques, our next goal is to test if selected functions of the coatings are compromised by the different treatments. More specifically, we first compare the wettability of the different samples (Figure 3a–c), which plays a key role for the antibiofouling and friction-reducing effects of mucin coatings.<sup>[9,11]</sup> A reliable quantification of the wetting behavior of a sample is provided by the static contact angle (CA) of a water droplet that is placed onto a sample surface: here, contact angles above 90° denote hydrophobic behavior, whereas contact angles smaller than 90° indicate hydrophilic surface properties. Exemplary images of droplets placed onto the different materials with and without covalent mucin coatings, respectively, are depicted in Figure 3d.

Our first observation is that, as expected, the wettability of the uncoated base materials differs. The CA values obtained for PU and PVC are located around the threshold between hydrophobic and hydrophilic behavior, whereas PDMS exhibit clear hydrophobic behavior with high contact angles around 110°. On all three materials, however, the mucin coatings decrease the contact angles by ≈40°–50°, which corresponds to an alteration of the surface properties into hydrophilic behavior. Remarkably, this strong alteration in the wetting properties is maintained for all materials after exposure to ethylene oxide; in addition, after irradiation with gamma or UV rays, coatings generated on PU or PVC still provide clearly hydrophilic properties as well. Autoclaving, in contrast, leads to a strong increase of the contact angles, and this result agrees with the findings discussed above, which illustrated that this particular sterilization method induces severe damage to the mucin macromolecules.

Even though determining CA values is a standard approach in material science, in the context of contact lenses, a more application-oriented characterization of their wetting behavior is used. Here, the liquid film BUT is determined as this measure is of high relevance for the performance of a contact lens on the cornea: maintaining a full tear film coverage on the lens without rupture between blinking is essential to ensure comfort and to protect the underlying tissue from harm. For uncoated, blank PDMS lenses (Figure 3e), we measure very small values below 1 s; in other words, the liquid film ruptures

immediately after removing the sample from the liquid. Contact lenses that are covalently coated with mucins, in turn, perform way better (Figure 3e): here, the measured BUT values are in the range of ≈38 s. After sterilization with ethylene oxide, the BUT still reaches 30 s, and the corresponding values are ≈20 s for AC,  $\gamma$ , or UV irradiation. Thus, all those values are much larger than the average duration of a human blinking period, which is ≈5 s.<sup>[36]</sup> Also, these results support our findings obtained from the CA measurements and demonstrate that all treatments maintain the wetting improvement brought about by the mucin coating—at least to a certain extent.

In addition to improving the wettability of surfaces, another important property brought about by mucins is providing lubricity. Mucins typically achieve this via a combination of two effects: sacrificial layer formation and hydration lubrication. On hydrophobic surfaces such as PDMS, sacrificial layer formation is primarily driven by the molecule's unglycosylated termini: since they are hydrophobic, they enable transient mucin adsorption onto hydrophobic surfaces but allow the adsorbed glycoprotein to become sheared off again under tribological stress. Owing to the covalent coupling of mucins to surfaces as performed in this study focusing on coatings of medical devices, however, this particular mechanism will be suppressed. In contrast, the second mechanism, hydration lubrication, should still be fully operable: as the densely glycosylated central region of the mucin glycoprotein can bind lots of water molecules, it maintains a surface-bound lubricating liquid film even under tribological loads and thus reduces friction.

To assess the lubricating abilities of sterilized mucin coatings, we perform tribological measurements with flat PDMS samples (see methods). For blank, uncoated PDMS samples (Figure 4a), we obtain a typical Stribeck's curve showing low friction coefficients in the regime of hydrodynamic lubrication only (i.e., at high sliding velocities, which correspond to blinking movements of the upper eye lid<sup>[37]</sup>). After a steep transition zone (mixed lubrication regime), the boundary lubrication regime is entered, which is most relevant for sliding speeds as they are expected to occur between a contact lens and the cornea;<sup>[38]</sup> here, very high friction coefficients around 1 are

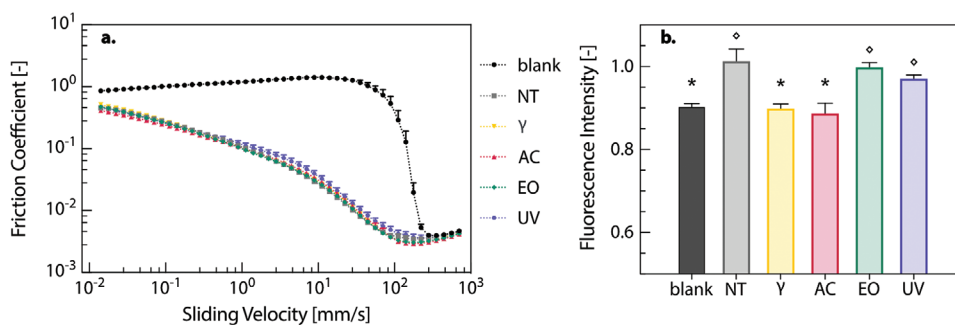


**Figure 4.** Tribological behavior and lipid adsorption as observed for mucin-coated PDMS samples. The Stribeck curves shown in (a) were obtained for PDMS samples that were either left uncoated (blank) or were covalently coated with mucin. The coated samples were either stored without any further treatment, or they were sterilized via  $\gamma$  irradiation, autoclaving, ethylene oxide fumigation, and UV irradiation, respectively. For all tribological data, a steel-on-PDMS material pairing was used in a rotational tribology setup (see the Experimental Section). Error bars denote the standard error of the mean as obtained from  $n = 4$  independent measurements per condition. The fluorescence intensities displayed in (b) were obtained in a lipid depletion assay. Higher values denote lower depletion of the lipids from the solution, hence lower adsorption of the lipids onto the sample surfaces. The error bars denote the standard error of the mean as obtained from  $n \geq 4$  samples. Asterisks and rhombi denote statistically significant differences between a treated sample and the untreated reference or the blank sample, respectively (based on a  $p$ -value of 0.05).

obtained. For mucin-coated samples, however, we find reduced friction coefficients across almost the whole range of sliding speeds probed. Now, instead of a steep transition from low to high friction coefficients, we observe a slow, gentle increase of friction with decreasing sliding speed. Even at the slowest sliding speed probed, the coated samples still outperform the uncoated ones. Remarkably, none of the sterilization methods tested here shows a measurable influence on the lubricity of the coating. With the previous results from the ELISA test and lectin assay in mind, this can be rationalized very well: As discussed above, the predominant lubrication mechanisms provided by covalent coatings is hydration lubrication, and this mechanism relies on the glycosylated parts of the mucin glycoprotein. As the results compiled in Figure 2 showed, the glycan pattern of mucins is more resilient toward the sterilization methods tested here than the unglycosylated, hydrophobic termini of mucin. Apparently, even with minor damages to this glycosylation pattern, the sterilized mucin layer can still bind sufficient amounts of water to provide hydration lubrication.

In addition to providing lubricity, a second key function established by mucin coatings is to counteract biofouling events, i.e., to reduce the undesired adsorption of molecules or cells onto surfaces.<sup>[9,11]</sup> For the medical devices studied here, this aspect is most relevant for contact lenses, which are optical devices that need to maintain a high transparency to allow for maximal light transmission. This property, however, can be drastically compromised by the deposition of molecules—typically lipids—that are present in the physiological tear film. Indeed, covalent mucin coatings have previously been shown to strongly reduce such lipid adsorption onto contact lenses,<sup>[12]</sup> thus preserving the transparency of the optical device. Hence, in a last set of experiments, we test if this lipid-repellent effect is still present after sterilization of the mucin coatings, and we conduct a depletion assay to assess this question (see the Experimental Section).

When exposing PDMS contact lenses to a lipid-rich liquid environment, we observe a substantially higher depletion of lipids for blank, uncoated samples than for unsterilized mucin-coated contact lenses (Figure 4b). Importantly, for the latter samples, the measured fluorescence values suggest that, here, lipid adsorption onto the coated contact lens surface is negligibly low. This finding is in full agreement with previous results and demonstrates the suitability of the employed depletion assay to study lipid deposition onto surfaces. Similarly, good results as those obtained for untreated coatings are also reached with coated samples that were either subjected to ethylene oxide or UV sterilization. After  $\gamma$ -irradiation or autoclavation, however, the outcome of this lipid deposition test is similar to that obtained for blank, uncoated PDMS lenses. Overall, these findings are consistent with the results obtained from the structural integrity tests shown in Figure 2d–f: Owing to the hydrophobic nature of PDMS, lipid adsorption can easily occur via hydrophobic interactions acting between the fatty acid chains of the lipids and the lens surface. For an intact mucin coating, the hydrophilic central region (which represents the largest part of the macromolecule) covers the surface and prevents the adsorption of hydrophobic objects. Accordingly, those sterilization methods that maintain the glycosylation pattern of the MUC5AC glycoprotein the best (i.e., ethylene oxide exposure, and UV treatment), also preserve the lipid-resistance properties of the coating.

## 4. Conclusion

The results discussed in this study show that, among the sterilization methods investigated here, mucin coatings are most robust toward ethylene oxide exposure; here, the biochemical integrity of the mucins and the properties brought about by the coating were maintained the best. One major concern associated with an ethylene oxide-based sterilization process, however, is the putative retention of toxic residues in the material. To enable clinical usage of medical products that have been subjected to ethylene oxide fumigation, the amount of such toxic residues needs to be minimized, which is typically achieved by extensive aeration of the treated devices after sterilization. Yet, the efficiency of different aeration methods (such as air circulation under heat, pulsed vacuum postprocessing, or microwave desorption) and the necessary duration or intensity of such post-sterilization treatments needs to be individually studied for each medical device. Moreover, even though lab-purified mucin macromolecules were shown to be highly biocompatible,<sup>[21]</sup> assessing the biocompatibility of mucin coatings before and after sterilization should be tested following detailed ISO protocols (including endotoxin tests) so mucin-coated medical devices can enter the next stage toward medical application.

Overall, the results obtained here for sterilized medical devices carrying a mucin coating are very positive as they indicate that making use of the various beneficial properties established by such mucin coatings should be very well possible in a clinical context: The three medical devices tested here find broad usage in many medical disciplines. Moreover, they represent an even broader range of objects made from the same set of polymeric materials, which can equally profit from the hydrophilizing, anti-biofouling, or friction-reducing effects brought about by such mucin coatings.

## Acknowledgements

The authors thank Matthias Marczyński for his kind assistance with the mucin purification. Furthermore, the authors thank Woehlk Contactlinsen GmbH for providing PDMS contact lenses. This research received funding from the German Federal Ministry for Economic Affairs and Energy through the Central Innovation Programme for small- and medium-sized enterprises (ZIM). Moreover, financial support from the Deutsche Forschungsgemeinschaft (DFG) through grant LI 1902/15-1 (project number 460209889) is gratefully acknowledged.

Open access funding enabled and organized by Projekt DEAL.

## Conflict of Interest

The authors declare no conflict of interest.

## Author Contributions

C.A.R., M.G.B., and O.L. designed the experiments. C.A.R. and J.C.H. performed the experiments and analyzed data. The manuscript was written by O.L. and C.A.R. All authors gave approval to the final version of the manuscript.



## Data Availability Statement

The data that support the findings of this study are available from the corresponding author upon reasonable request.

## Keywords

autoclavation, contact lens, endotracheal tube, ethylene oxide, gamma irradiation, urinary catheter, UV irradiation

Received: September 8, 2021

Revised: October 26, 2021

Published online: December 5, 2021

- 
- [1] P. J. Featherstone, C. M. Ball, R. N. Westhorpe, *Anaesth. Intensive Care* **2015**, 43, 435.
- [2] Z. K. Zander, P. Chen, Y.-H. Hsu, N. Z. Dreger, L. Savariou, W. C. Mcroy, A. E. Cerchiari, S. D. Chambers, H. A. Barton, M. L. Becker, *Biomaterials* **2018**, 178, 339.
- [3] P. Poli, A. Scocca, F. Di Puccio, G. Gallone, L. Angelini, E. M. Calabrò, *J. Vasc. Access* **2016**, 17, 175.
- [4] A. Victor, J. E. Ribeiro, F. Araújo, *J. Mech. Eng. Biomech.* **2019**, 4, 1.
- [5] B. Y. Yoo, B. H. Kim, J. S. Lee, B. H. Shin, H. Kwon, W.-G. Koh, C. Y. Heo, *Acta Biomater.* **2018**, 76, 56.
- [6] H. R. Thorarinsdottir, T. Kander, A. Holmberg, S. Petronis, B. Klarin, *Crit. Care* **2020**, 24, 1.
- [7] P. Singha, J. Locklin, H. Handa, *Acta Biomater.* **2017**, 50, 20.
- [8] H. Liu, S. Shukla, N. Vera-González, N. Tharmalingam, E. Mylonakis, B. B. Fuchs, A. Shukla, *Fron. Cell. Infect. Microbiol.* **2019**, 9, 37.
- [9] B. Winkeljann, M. G. Bauer, M. Marczynski, T. Rauh, S. A. Sieber, O. Lieleg, *Adv. Mater. Interfaces* **2020**, 7, 1902069.
- [10] J. Song, B. Winkeljann, O. Lieleg, *Adv. Mater. Interfaces* **2020**, 7, 2000850.
- [11] J. Song, T. M. Lutz, N. Lang, O. Lieleg, *Adv. Healthcare Mater.* **2021**, 10, 2000831.
- [12] C. A. Rickert, et al, *ACS Appl. Mater. Interfaces* **2020**, 12, 28024.
- [13] D. A. Dartt, *Prog. Retinal Eye Res.* **2002**, 21, 555.
- [14] S. K. Linden, P. Sutton, N. G. Karlsson, V. Korolik, M. A. Mcguckin, *Mucosal Immunol.* **2008**, 1, 183.
- [15] A. P. Corfield, *Biochim. Biophys. Acta, Gen. Subj.* **2015**, 1850, 236.
- [16] J. A. Voynow, B. K. Rubin, *Chest* **2009**, 135, 505.
- [17] D. J. Thornton, K. Rousseau, M. A. Mcguckin, *Annu. Rev. Physiol.* **2008**, 70, 459.
- [18] M. E. V. Johansson, G. C. Hansson, *Nat. Rev. Immunol.* **2016**, 16, 639.
- [19] R. Bansil, B. S. Turner, *Curr. Opin. Colloid Interface Sci.* **2006**, 11, 164.
- [20] V. J. Schömig, B. T. Käs Dorf, C. Scholz, K. Bidmon, O. Lieleg, S. Berensmeier, *RSC Adv.* **2016**, 6, 44932.
- [21] O. Lieleg, C. L. L. Bloom, C. B. Buck, K. Ribbeck, *Biomacromolecules* **2012**, 13, 1724.
- [22] H. Yan, C. Seignez, M. Hjorth, B. Winkeljann, M. Blakeley, O. Lieleg, M. Phillipson, T. Crouzier, *Adv. Funct. Mater.* **2019**, 29, 1902581.
- [23] W. A. Rutala, D. J. Weber, *Am. J. Infect. Control* **2013**, 41, S2.
- [24] N. P. Tipnis, D. J. Burgess, *Int. J. Pharm.* **2018**, 544, 455.
- [25] S. Ray, R. P. Cooney, *Handbook of Environmental Degradation of Materials*, **2018**, Elsevier, Amsterdam pp. 185–206.
- [26] E. V. Khoroshilova, Y. A. Repeyev, D. N. Nikogosyan, *J. Photochem. Photobiol., B* **1990**, 7, 159.
- [27] J. A. Reisz, et al, *Antioxid. Redox Signaling* **2014**, 21, 260.
- [28] K. Funatsu, H. Kiminami, Y. Abe, J. F. Carpenter, *J. Pharm. Sci.* **2019**, 108, 770.
- [29] L. Chen, C. Sloey, Z. Zhang, P. V. Bondarenko, H. Kim, D. a R. Sekhar Kanapuram, *J. Pharm. Sci.* **2015**, 104, 731.
- [30] M. Marczynski, K. Jiang, M. Blakeley, V. Srivastava, F. Vilaplana, T. Crouzier, O. Lieleg, *Biomacromolecules* **2021**, 22, 1600.
- [31] B. Winkeljann, P.-M. A. Leipold, O. Lieleg, *Adv. Mater. Interfaces* **2019**, 6, 1900366.
- [32] J. T. Gallagher, M. Harding, R. E. Dale, *Proc. of the Fifth Lectin Meet. Bern, De Gruyter, Berlin* **1982**,
- [33] K. Boettcher, S. Grumbein, U. Winkler, J. Nachtsheim, O. Lieleg, *Rev. Sci. Instrum.* **2014**, 85, 093903.
- [34] M. B. Abelson, I. J. Udell, J. H. Weston, *Arch. Ophthalmol.* **1981**, 99, 301.
- [35] B. T. Käs Dorf, F. Weber, G. Petrou, V. Srivastava, T. Crouzier, O. Lieleg, *Biomacromolecules* **2017**, 18, 2454.
- [36] L. G. Carney, R. M. Hill, *Acta Ophthalmol.* **1982**, 60, 427.
- [37] M. G. Doane, *Am. J. Ophthalmol.* **1980**, 89, 507.
- [38] A. C. Dunn, J. A. Tichy, J. M. Urueña, W. G. Sawyer, *Tribol. Int.* **2013**, 63, 45.